ACS Catalysis

Boosting up the Low Catalytic Activity of Silver for H$_2$ Production on Ag/TiO$_2$ Photocatalyst: Thiocyanate as a Selective Modifier

Yeoseon Choi, Hyoung-il Kim, Gun-hee Moon, Seongwon Jo, and Wonyong Choi*

Department of Chemical Engineering and School of Environmental Science and Engineering, Pohang University of Science and
Technology (POSTECH), Pohang 790-784, Republic of Korea

Ⓢ Supporting Information

ABSTRACT: Noble metal cocatalysts like Pt have been
widely employed as an essential ingredient in many kinds of
photocatalytic materials for solar hydrogen production. The
high material cost of Pt is the biggest limitation. Silver is far
less expensive but much less active than Pt and Au as a
hydrogen evolving catalyst. Here we demonstrate a new
strategy to boost up the activity of silver in Ag/TiO$_2$ for
photocatalytic H$_2$ production via forming a simple surface
complexation of thiocyanate (SCN$^-$) on silver. The addition of
thiocyanate in the suspension of Ag/TiO$_2$ markedly enhanced
the photocatalytic production of H$_2$ by about 4 times.
Thiocyanate was not consumed at all during the photoreaction, which ruled out the role of thiocyanate as an electron donor.
Such a positive role of thiocyanate was not observed with bare TiO$_2$, Pt/TiO$_2$, and Au/TiO$_2$. The selective chemisorption of
thiocyanate on silver was confirmed by the analyses of Raman spectroscopy and spot-profile energy-dispersive spectroscopy. In
the presence of thiocyanate, the overpotential for water reduction on Ag/TiO$_2$ electrode was slightly reduced, and the interfacial
charge transfer resistance on Ag/TiO$_2$ (measured by electrochemical impedance spectroscopy) was significantly decreased,
whereas other electrode systems (bare TiO$_2$, Au/TiO$_2$, and Pt/TiO$_2$) showed the opposite effect of thiocyanate. These results
indicate that the adsorption of thiocyanate on Ag facilitates the transfer of photogenerated electrons on the Ag/TiO$_2$ electrode. It
is proposed that the formation of Ag-SCN surface complex enhances the interfacial electron transfer rate and facilitates the
reduction of protons on Ag/TiO$_2$.

KEYWORDS: silver-loaded TiO$_2$, photocatalysis, hydrogen evolution, thiocyanate complex, photoinduced electron transfer
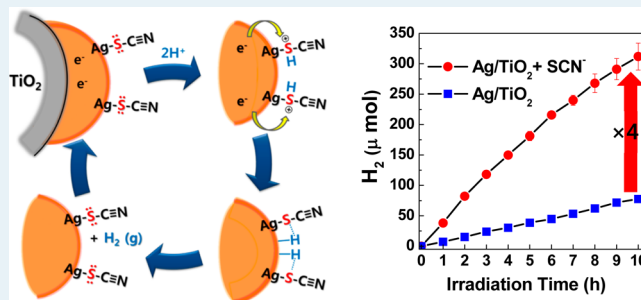
1. INTRODUCTION

Utilizing solar energy to produce hydrogen from water splitting
is a challenging topic, and the key issue is centered on how to
produce hydrogen efficiently using stable and low-cost
materials.[1−4] TiO$_2$ has been widely used as a base material
for this purpose since the first report of a H$_2$-producing
photoelectrochemical system employing TiO$_2$ as a photo-
anode[5] because of its excellent stability in aqueous environ-
ment, abundance, and low material cost.[6−10] However, the fast
charge recombination in TiO$_2$ should be overcome to enhance
its photoconversion efficiency.[7,11] One of the common
methods to retard the recombination and to enhance the
charge separation efficiency (hence the photocatalytic activity)
is to load noble metal nanoparticles on the surface of
photocatalysts,[12−14] which forms a Schottky junction at the
semiconductor/metal interface.[15−17]

A noble metal on semiconductor photocatalysts helps to
separate the photoinduced charge pairs by attracting electrons,
to facilitate the interfacial electron transfer, and to catalyze the
production of molecular hydrogen on its surface.[18−21] Although
these noble metals (e.g., Pt, Au, and Pd) have been widely
employed as a surface modifier of TiO$_2$ and other semi-
conductors,[18,22−26] they are rare and expensive, which severely

limits their practical applications. Therefore, the development
of lower-cost materials should be achieved to make the solar
hydrogen production more practical. In this respect, silver (Ag)
is an attractive alternative because of its much lower material
cost (70 times lower than Au and Pt and 50 times lower than
Pd) but is much less effective than Pt and Au as a catalyst for
hydrogen production.[27,28]

According to the volcano plot of hydrogen evolution on
metal catalysts, the hydrogen evolution reaction (HER) on
silver is limited by its lower binding energy (metal−hydrogen
bond).[29] The bond strength of Ag−H (37 kcal/mol) is much
weaker than that of Pt−H (60 kcal/mol) and Au−H (45 kcal/
mol).[29] Another possible reason for lower efficiency of Ag than
Pt is the slow interfacial electron transfer.[30−32] In other words,
electrons injected in the silver phase are accumulated with the
retarded interfacial transfer. Therefore, the cocatalytic activity
of Ag would be enhanced by the surface modification that
facilitates proton binding and electron transfer.

The silver surface has a strong affinity for sulfur compounds.[33−37] Thiocyanate is a pseudohalide anion which is strongly electronegative and easily adsorbs on silver.[38] Herein we report that the photocatalytic hydrogen production on Ag/TiO$_2$ is highly enhanced in the presence of thiocyanate, which does not undergo any chemical transformation during the photoreaction, while such a positive effect of thiocyanate is not observed at all with Pt/TiO$_2$ and Au/TiO$_2$. Thiocyanate formed a surface complex on silver and facilitated the photoreduction of protons to molecular hydrogen on the illuminated Ag/TiO$_2$.

2. EXPERIMENTAL SECTION

2.1. Preparation of the Ag/TiO$_2$ Nanocomposite. Ag nanoparticles (NPs) were loaded onto the surface of TiO$_2$ (P25) by using a typical photodeposition method. An aqueous suspension of titanium dioxide (0.5 g L^{-1}) with 1 M methanol (as an electron donor) and 0.14 mM silver nitrate (AgNO$_3$, 99.9% ACS reagent) was stirred and sonicated for 30 min before the irradiation. After irradiation with a 200 W mercury lamp for 30 min, the Ag-loaded TiO$_2$ was filtered, washed with distilled water, and dried in an oven at 80 °C. Pt/TiO$_2$ and Au/TiO$_2$ were prepared in the same way by using chloroplatinic acid (H$_2$PtCl$_6$, Aldrich) and chloroauric acid (HAuCl$_4$, Sigma-Aldrich) as the metal precursor, respectively.[39] A typical metal loading was estimated to be ca. 3.0 wt % (for Ag/TiO$_2$, Pt/TiO$_2$, Au/TiO$_2$) by measuring the unused precursor concentration after the photodeposition using inductively coupled plasma-atomic emission spectroscopy (ICP-AES, Spectro).

Ag/TiO$_2$ powder adsorbed with thiocyanate was prepared for the analyses of high-resolution transmission electron micrographs (HR-TEM), Raman spectroscopy, diffuse reflectance UV−vis absorption spectra (DRS), and X-ray photoelectron spectroscopy (XPS). In order to analyze characteristics of Ag-SCN/TiO$_2$, sample was prepared by adding a calculated amount of potassium thiocyanate (KSCN) in the aqueous suspension of Ag/TiO$_2$ and stirred for 3 h. The suspension was filtered without additional washing and then dried in an oven at 80 °C. Ag/TiO$_2$ powder was also prepared in a similar way in the absence of thiocyanate as a control sample.

2.2. Photocatalytic Hydrogen Generation. The prepared Ag/TiO$_2$ was resuspended in an aqueous solution of methanol (as an electron donor) and potassium thiocyanate in a pyrex reactor. The suspension was dispersed well by ultrasonication and purged with argon in a sealed reactor prior to illumination. A 300 W Xe arc lamp (Oriel) was used as a light source, and the light was passed through a 10 cm IR water filter and a UV cutoff filter ($\lambda > 320$ nm). During irradiation, the head space gas (∼35 mL) of the reactor was intermittently sampled and analyzed for H$_2$ using a gas chromatograph (Agilent 6890A) equipped with a thermal conductivity detector and a 5 Å molecular sieve column. The photocatalytic hydrogen production in the same batch reactor was repeated by purging the reactor with argon gas at the end of each photoirradiation cycle (3 h) and before starting the next cycle.

2.3. Characterization of Photocatalysts. Ag NPs distribution over TiO$_2$ particles was characterized using scanning transmission electron microscopy (STEM) and high-angle annular dark-field (HAADF), and the elemental distribution was analyzed by energy dispersive X-ray spectroscopy (EDS), all of which were carried out using a JEOL JEM-2200FS with image Cs-corrector (200 keV, 0.1 nm). Diffuse

reflectance UV−vis absorption spectra were recorded using a spectrophotometer (Shimadzu UV-2401PC) with an integrating sphere attachment. BaSO$_4$ was used as the reference. The surface atomic compositions of Ag/TiO$_2$ adsorbed with thiocyanate were determined by X-ray photoelectron spectroscopy (XPS) (Kratos XSAM 800pci) using the Mg Kα line (1253.6 eV) as an excitation source. A Raman spectrometer (Horiba Jobin Yvon/LabRam Aramis) was employed to analyze the stretching vibration of SCN$^-$ adsorbed on Ag/TiO$_2$ using the 514 nm laser line (Ar-ion laser) as the excitation source. Thiocyanate adsorption and degradation was monitored by using an ion chromatograph (IC, Dionex DX-120) that was equipped with a Dionex IonPac AS 16 (4 mm × 250 mm) column and a conductivity detector.

2.4. Photoelectrochemical Measurements. Photoelectrochemical (PEC) measurements were performed using a potentiostat (Gamry, Reference 600) that was connected to a conventional three-electrode PEC reactor (Pyrex cell with a quartz window). A photocatalyst loaded Ti foil, coiled Pt wire, and Ag/AgCl electrode were used as a working, a counter, and a reference electrode, respectively. The photocatalyst electrodes were prepared by using an electrophoretic method.[40] Titanium foil (thickness 0.127 mm, 99.7%, Aldrich) was used as a substrate for the electrophoretic deposition of photocatalyst. An anode Ti-foil was masked off using an insulating tape to expose an area of 1 cm^2 and a bare Ti-foil was used as a cathode in the electrophoretic deposition. The two Ti foil electrodes were immersed in the suspension of P25 or M/TiO$_2$ (M = Pt, Au, Ag) (10 g/L) in pure methanol, electrically connected, and then 25.0 V was applied to the Ti-foil electrodes for 25 s for electrodeposition. The anode Ti-foil was then removed from the suspension and calcined at 450 °C for 30 min under Ar flow. Although the M/TiO$_2$ electrodes were treated at higher temperature than the M/TiO$_2$ powder samples (450 °C vs 80 °C), the surface oxidation state of metal and TiO$_2$ crystallinity remained the same according to XPS and X-ray diffraction analysis. The three-electrode PEC reactor contained an aqueous electrolyte solution consisting of NaClO$_4$ (0.2 M) and methanol (10 vol %) at pH 11.0, which was continuously purged with Ar gas. Linear sweep voltammogram (LSV) and electrochemical impedance spectroscopy (EIS) were measured at applied bias from −2.0 to 1.5 V, and −1.0 V (vs Ag/AgCl), respectively. The open-circuit potential (OCP) was also measured in NaClO$_4$ (0.2 M) electrolyte at pH 11.0. The open-circuit stationary potential in the dark (E_0) and under UV irradiation (E_{ph}) was measured after 1000 s to allow enough time for equilibration.[41] To ensure the reproducibility of the electrode behavior, the same electrode was used in the PEC measurements. The same 300 W Xe arc lamp (Oriel) was also used in the PEC measurement as a light source as in the photocatalysis experiments.

3. RESULTS AND DISCUSSION

Noble metal NPs (Ag, Pt, and Au) were loaded (typically ∼3 wt %) onto the surface of TiO$_2$ (P25) by using a typical photodeposition method. The addition of thiocyanate in the suspension of Ag/TiO$_2$ (in the presence of methanol (MeOH) as an electron donor) markedly enhanced the photocatalytic production of H$_2$ by about 4 times, as shown in Figure 1a. The presence of MeOH as a sacrificial electron donor was essential for the production of H$_2$, and the presence of thiocyanate alone without MeOH did not induce the production of H$_2$ on Ag/TiO$_2$ at all. This indicates that the role of thiocyanate is not the

(a)

(b)
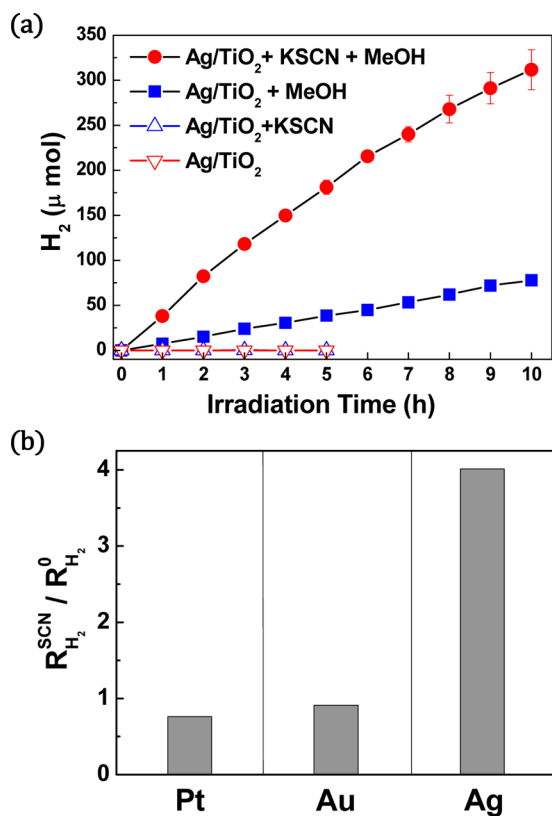
Figure 1. (a) Time profiles of photoproduction of H_2 on Ag-loaded TiO_2 with and without SCN^-. (b) Comparison of SCN^- effect among Pt/TiO_2, Au/TiO_2, and Ag/TiO_2 in terms of the relative ratio of thiocyanate effect on H_2 production (R_{H2}^0 and R_{H2}^{SCN}: H_2 production rate without and with thiocyanate, respectively). The experiments were tested under the condition of: [catalyst] = 0.5 g/L, [MeOH] = 10 vol %, [SCN^-] = 0.1 mM, pH = 7, initially Ar-saturated, and λ > 320 nm irradiation.

electron donor (or hole scavenger).[42−44] On the other hand, such positive effect of thiocyanate was not observed at all with Pt/TiO_2 and Au/TiO_2 (see Figure 1b and Figure S1): the H_2 generation efficiency was reduced (for Pt) or little changed (for Au) in the presence of thiocyanate. The positive thiocyanate effect on the H_2 production was also observed in the presence of other electron donors such as ethanol and ethylenediaminetetraacetic acid (EDTA) instead of MeOH (see Figure 2a). The thiocyanate effect was optimized by varying [KSCN] and silver loading (see Figure 2b,c), which shows that the effect is saturated at [KSCN] > 0.1 mM and Ag loading > 3.0 wt %. Therefore, most tests in this work were carried out with Ag (3.0 wt %)/TiO_2 and 0.1 mM KSCN. It should be noted that the thiocyanate effect on H_2 production reaches a saturation at around [KSCN] = 0.1 mM, which coincides with the saturation point of thiocyanate adsorption on Ag/TiO_2 (see Figure 2b). On the other hand, thiocyanate was little adsorbed on Pt/TiO_2, Au/TiO_2, and bare TiO_2 (see Table 1), which clearly indicates that thiocyanate strongly interacts with Ag NPs and the surface complexation of thiocyanate on Ag/TiO_2 should be responsible for the enhancement of H_2 production. The concentration of thiocyanate was not reduced at all during the photoirradiation (see Figure 2d), which indicates that the photocatalytic degradation of thiocyanate through its reaction with holes and hydroxyl radicals was inhibited in the presence of excess hole scavengers (MeOH).

To further confirm the thiocyanate effect, several control tests were also carried out and shown in Figure 3a. Regardless of the kind of counter cations, the tested thiocyanate reagents (i.e., GSCN (guanidium thiocyanate), NaSCN, and KSCN) all showed the same positive effects, which rules out any possible role of counter cations. The structurally similar anions of cyanide (CN^-) and cyanate (OCN^-) that do not contain a sulfur atom minimally improved the activity of H_2 generation on Ag/TiO_2. This reassures that the observed enhancement effect of thiocyanate should be ascribed to the unique interaction between Ag/TiO_2 and thiocyanate ions. It should be noted that the thiocyanate-enhanced production of H_2 on Ag/TiO_2 was largely maintained through the repeated cycles of photocatalysis with showing little sign of deactivation (Figure 3b). Although the silver deposited on TiO_2 may undergo oxidative dissolution via reaction with holes under illumination, the presence of excess MeOH as a reductant should inhibit such dissolution reaction.

STEM images (Figure 4) show that Ag NPs (bright sphere in the dark field STEM) are well deposited on the host TiO_2 particles, and the average size of Ag NPs is about 4 nm (ranging 1−20 nm). Pt and Au NPs are also well deposited on TiO_2 particles (see Figure S2) but somewhat differ from Ag NPs in their sizes. Pt NPs are smaller (1−3 nm) than Ag NPs, whereas Au NPs are larger (3−28 nm) than Ag NPs. Although the different sizes of noble metal NPs may have some effect on the photocatalytic activity, the present study is focused on the relative effect of thiocyanate in metal-loaded TiO_2, which should not be critically influenced by the different sizes of metal NPs. To confirm the adsorption of SCN^- on Ag/TiO_2, spot-profile EDS (energy dispersive X-ray spectroscopy) method was used and the analysis results for Ag/TiO_2 and thiocyanate-adsorbed Ag/TiO_2 are summarized in Figure 4e (see Figure S3 for EDS spectra). The spot-profile EDS confirmed that the white bright spheres are Ag NPs and larger irregularly shaped particles are TiO_2. The element sulfur was detected significantly only on the thiocyanate-adsorbed Ag/TiO_2, and mainly on the region of Ag NPs, which indicates that thiocyanate is preferentially located on Ag not TiO_2. In addition, the adsorption of thiocyanate on silver surface reduced the intensity of Ag band in the X-ray photoelectron spectrum of Ag/TiO_2 (see Figure S4).

A more convincing evidence for the direct interaction between thiocyanate and silver surface is obtained from the Raman spectral analysis (Figure 5a). The main Raman signal for free thiocyanate is located at 2070 cm^{-1}, which is attributed to the stretching vibration of C≡N bond. The free thiocyanate spectrum was measured in aqueous solution, and the broad peak at 1640 cm^{-1} results from the symmetric bending mode of water.[45] All the other spectra in Figure 5a were measured in solid state. When thiocyanate is adsorbed on Ag/TiO_2, the peak was shifted to higher frequency (2130 cm^{-1}), which implies that the bond strength of C≡N increases upon adsorption on Ag/TiO_2. The Raman frequency of 2130 cm^{-1} is identical to that reported for thiocyanate adsorbed on colloidal silver particles.[38] The π-electrons in the C≡N bond in free thiocyanate is delocalized with the p-electrons on S atom. However, when thiocyanate adsorbs on Ag surface via S atom, the delocalization of π-electrons is hindered, and the π-electrons in the C≡N bond are more localized with enhancing its vibration frequency. Note that such thiocyanate Raman signal is absent or insignificant with bare TiO_2, Pt/TiO_2, and Au/TiO_2, which indicates that the strong binding of
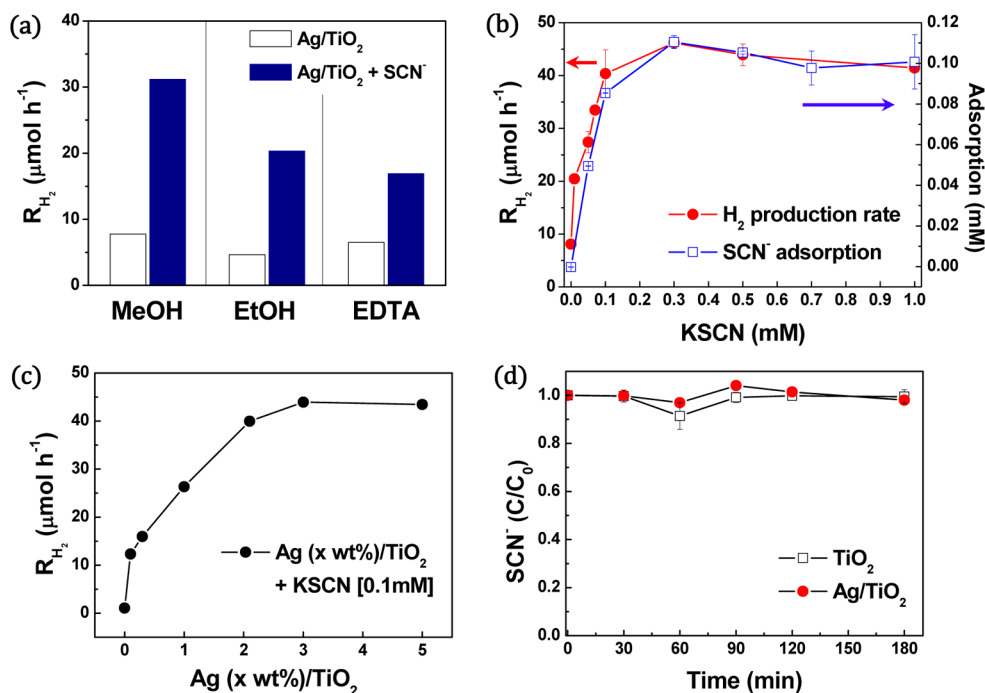
Figure 2. (a) Rate of hydrogen generation, R_{H_2} (μmol/h) in the presence of different electron donors (methanol, ethanol, and EDTA) (b) Rate of H_2 production (left axis) and the adsorbed amount of SCN^- on Ag (3.0 wt %)/TiO_2 (right axis) as a function of added KSCN concentration. (c) H_2 production rate as a function of Ag loading on TiO_2. (d) Time profiles of SCN^- concentration monitored during the UV irradiation of the catalyst suspension (Ag/TiO_2 (or TiO_2) + KSCN + MeOH). The experiment conditions were [catalyst] = 0.5 g/L, [ED] = 10 vol % ([EDTA] = 10 mM), initially Ar-saturated, and λ > 320 nm irradiation.

Table 1. Adsorption of Thiocyanate on Bare TiO_2 and Metal-Loaded (3 wt %) TiO_2

| photocatalyst (PC)	Ag/TiO_2	Pt/TiO_2	Au/TiO_2	TiO_2
adsorbed SCN^- on PC (μmol/g·cat)[a]	220	24	8	8

[a]Uncertainty of $\pm$2 μmol/g·cat.

thiocyanate on the noble metal surface is unique with the Ag/TiO_2 sample, which should be responsible for the marked positive effect of thiocyanate on the photocatalytic hydrogen production. In addition, diffuse reflectance UV−vis spectra (DRS) also gave an evidence for the strong interaction between Ag-SCN. With the adsorption of thiocyanate, the plasmon peak of Ag NPs on TiO_2 was blue-shifted, and the intensity was also diminished at the same time (see Figure 5b). This indicates that the thiocyanate adsorption changes the electron density at the silver surface. The blue-shift of silver plasmon band can be ascribed to the fact that the adsorption of sulfur compounds on Ag NPs can increase the electron density of silver surface.[31,46] However, such spectral shift was not clearly observed (or very minor) with Ag-OCN, Au-SCN, and Au-OCN systems, which is consistent with the peculiar strong surface interaction of Ag-SCN (see Figure 5a and Table 1). The thiocyanate-induced spectral blue shift of the silver plasmonic band was also recently observed and investigated for its application to optical thiocyanate sensor.[47]

The positive effect of thiocyanate on the hydrogen production on Ag/TiO_2 implies that the presence of thiocyanate should facilitate the electron transfer to protons. The photoelectrochemical (PEC) characteristics of Ag/TiO_2 and other electrodes are compared in Figure 6. The PEC experiments were carried out in the similar condition of

photocatalytic H_2 production. In the linear sweep voltammogram (LSV) of Figure 6a, it is clearly shown that the presence of noble metals (Ag, Au, and Pt) markedly reduces the overpotential of H_2 production, of which efficiency is in the order of Ag < Au < Pt, which is well-known.[1,28] In the presence of thiocyanate, the onset potential for water reduction on Ag/TiO_2 electrode was slightly shifted to the positive direction (hence less overpotential for H_2 production), whereas other electrode systems (bare TiO_2, Au/TiO_2, and Pt/TiO_2) showed the opposite trend upon adding thiocyanate. This is consistent with the observation that only Ag/TiO_2 exhibited the enhanced photocatalytic production of H_2 in the presence of thiocyanate. Charge transfer properties under proton reduction potential (−1.0 V) and UV irradiation were measured by electrochemical impedance spectroscopy (EIS). Resistance was generated by charge transfer in the bulk and interfacial layer, electrical double layer, ions diffusion, methanol and its intermediates oxidation reaction and other various subeffects. Figure 6b shows that EIS Nyquist plots of Ag, Au, and Pt/TiO_2 with and without SCN^-. A simple model of connecting two Randles circuits (at the high and low frequency) in series was used for data fitting. The resistance of the first arc (R_1) and the second arc (R_2) on Ag/TiO_2 was significantly reduced in the presence of thiocyanate in the irradiated condition, whereas R_1 and R_2 of Pt/TiO_2 and Au/TiO_2 increased in the presence of thiocyanate (see Figure 6c). Both LSV and EIS results indicate that the adsorption of thiocyanate on Ag facilitates the transfer of photogenerated electrons on the Ag/TiO_2 electrode.
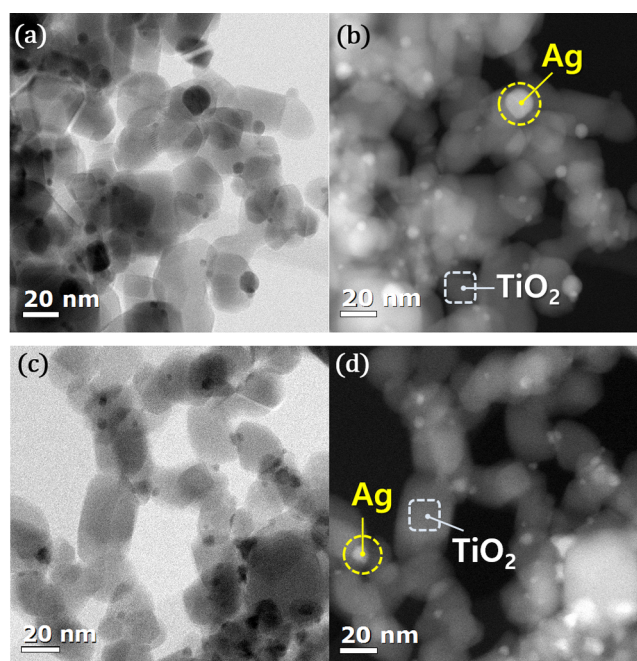
Figure 7a compares the open-circuit stationary values of TiO_2 and M/TiO_2 (M= Pt, Au, and Ag) electrodes. The illuminated electrode (n-type semiconductor) accumulates electrons on it, so the open-circuit potential (OCP) shifted negatively until it reaches a photostationary potential (E_{ph}).[41,48]
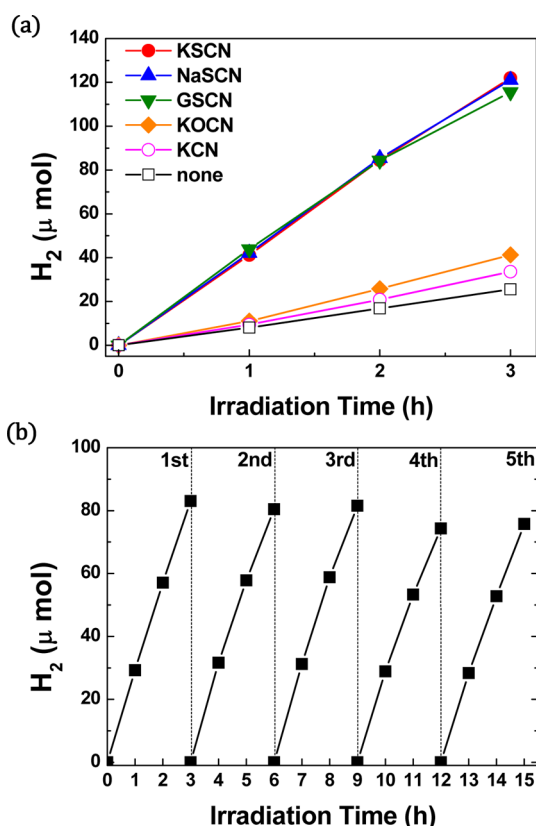
Figure 3. (a) Control experiments to confirm SCN^- effect with using test reagents that are structurally similar to thiocyanate. (b) Repeated photocatalysis runs of H_2 generation with Ag (3.0 wt %)/TiO_2 in the presence of SCN^-. Hydrogen gas was purged every 3 h without replenishing any chemical reagents.The experiments were tested under the condition of the following: [catalyst] = 0.5 g/L, [MeOH] = 10 vol %, [SCN^-] = 0.1 mM, pH = 7, initially Ar-saturated, and λ > 320 nm irradiation.

(e)

Sample	Spot	O	Ti	Ag	S
Ag/TiO_2	Ag	33	36	31	0
	TiO_2	58	42	0	0
Ag/TiO_2 + KSCN	Ag	36	43	19	2.0
	TiO_2	37	63	0	0

* Unit: atom% (uncertainty of ± 0.5%)

Figure 4. Bright-field and dark-field images of STEM for (a,b) bare Ag/TiO_2 and (c,d) thiocyanate-adsorbed Ag/TiO_2. (e) The atom% of oxygen (O), titanium (Ti), silver (Ag), and sulfur (S) at the marked spots of Ag NP and TiO_2 was measured by spot-profile EDS. Sulfur was predominantly found on the Ag spot in SCN^- adsorbed Ag/TiO_2.

E_{ph} is related to quasi-Fermi level, which is an equilibrium state of excess electrons.[41,49,50] Figure 7a displays that E_{ph} is not much influenced by the presence of thiocyanate, which means that the potential for reducing protons was not influenced by thiocyanate.

Dark stationary potential (E_0) is related to Fermi level of electrode, which directly reflects the potential at the electrode/electrolyte interface.[50] Pt/TiO_2 electrode exhibits a markedly positive stationary potential in the dark, which might be ascribed to the preferential adsorption of protons (H^+) on Pt surface and the strong surface binding affinity of Pt−H. On the other hand, E_0 of Ag/TiO_2 and Au/TiO_2 is only slightly shifted to the positive direction from that of bare TiO_2, which is consistent with less catalytic activity of Ag and Au than Pt. It should be noted that the effect of thiocyanate addition on E_0 is markedly different between Ag/TiO_2 and other electrodes. E_0 shifted to the negative direction upon the addition of thiocyanate anions with bare TiO_2, Au/TiO_2, and Pt/TiO_2, whereas it moved to the positive direction with Ag/TiO_2 on the contrary. This implies that the strong surface complex formation of thiocyanate on the silver surface facilitates the proton adsorption on Ag surface with making the surface potential more positive, whereas the presence of thiocyanate in the electrolyte hinders (or little change) the adsorption of protons on TiO_2, Pt, and Au.
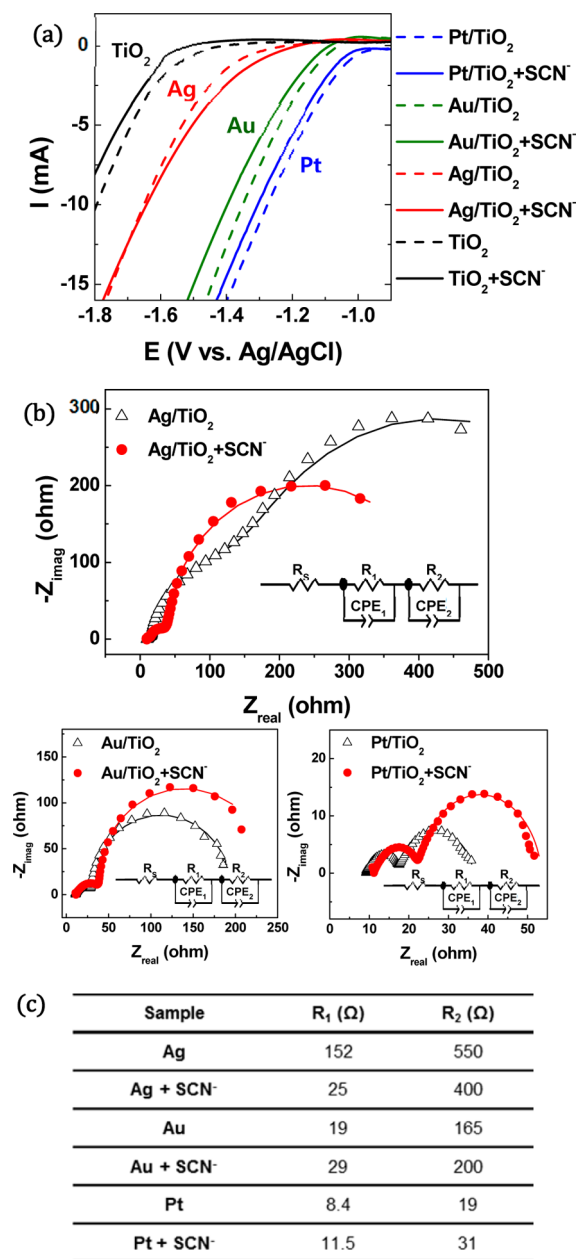
The OCP decay (see Figure 7b) upon turning off the light reflects the slow surface recombination process in the electrode. In comparing TiO_2 and M/TiO_2 (M = Pt, Au, and Ag), OCP decay rate decreased in the order of TiO_2 > Ag/TiO_2 > Au/TiO_2 > Pt/TiO_2, which is inversely correlated with the hydrogen production activity. Pt/TiO_2 has the highest activity of hydrogen production because it exhibits the slowest charge recombination. It should be noted that the effect of thiocyanate on the OCP decay is also unique with Ag/TiO_2 compared with other systems. The presence of thiocyanate markedly retarded the OCP decay rate with Ag/TiO_2 electrode, whereas the thiocyanate effect on Au/TiO_2 and Pt/TiO_2 is minimal or the opposite. In particular, the addition of thiocyanate in the Pt/TiO_2 system greatly accelerated the OCP decay rate, which explains why thiocyanate reduced the hydrogen production on Pt/TiO_2 (see Figure 1b).

The above experimental evidence show that thiocyanate is selectively chemisorbed on the silver surface and uniquely influences the charge transfer process on it. Being an electronegative pseudohalide ion, the surface-complexed thiocyanate withdraws electrons from silver, and at the same time the nonbonding electrons on the sulfur atom provide the Lewis base sites for proton uptake. It should be noted that the addition of hydrosulfide ion (HS^-) instead of thiocyanate in the

(a)

(b)
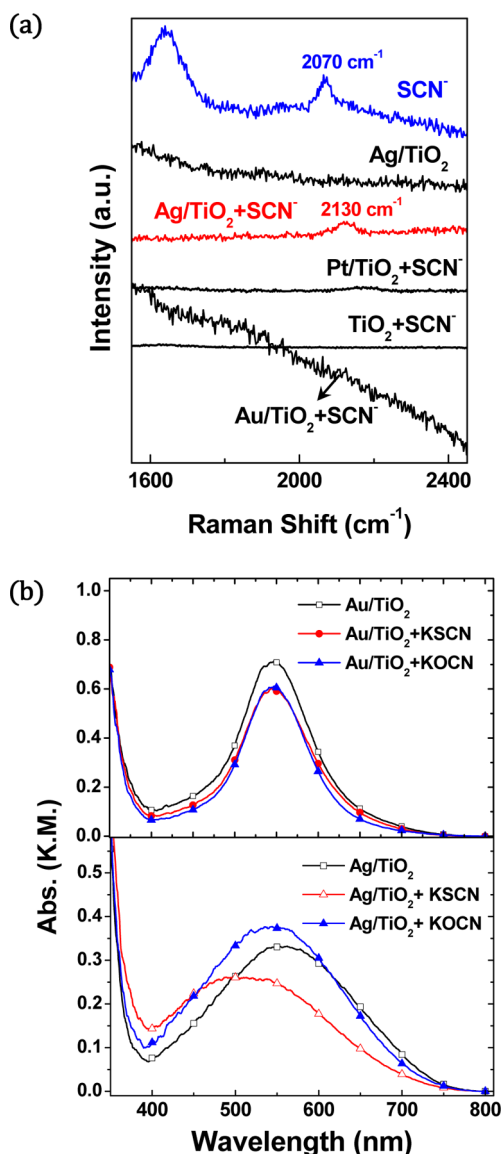
Figure 5. (a) Raman spectra of thiocyanate adsorbed on various photocatalyst samples (bare TiO_2, Ag/TiO_2, Pt/TiO_2, Au/TiO_2) compared with free thiocyanate. (b) Diffuse reflectance UV–vis spectra of Ag/TiO_2 and Au/TiO_2 and their spectral change upon the adsorption of SCN^- and OCN^-.

(a)

(b)

(c)

Sample	R_1 (Ω)	R_2 (Ω)
Ag	152	550
Ag + SCN^-	25	400
Au	19	165
Au + SCN^-	29	200
Pt	8.4	19
Pt + SCN^-	11.5	31

Figure 6. (a) Linear sweep voltammograms (LSV) at scan rate 10 mV/s for the electrode of bare TiO_2, Ag/TiO_2, Pt/TiO_2, Au/TiO_2. (b) Electrochemical impedance spectroscopy (EIS) Nyquist plots were obtained in the frequency range of 5 mHz to 100 kHz under UV-light irradiation to compare the effect of thiocyanate. (c) R_1 and R_2 estimated from EIS result. [$NaClO_4$] = 0.2 M, [MeOH] = 10 vol %, pH = 11.0, electrode area of 1 cm^2, λ > 320 nm. Applied bias for photocurrent and EIS are 0.5 V and −1.0 V (vs Ag/AgCl), respectively.

Ag/TiO_2 suspension did not enhance the hydrogen production activity at all, which implies that the sulfur adsorption on Ag surface is not sufficient to enhance the photocatalytic H_2 production. The presence of the CN group, which is highly electron-withdrawing, seems to be essential to facilitate the interfacial electron transfer. Therefore, the combined effects of S and CN in thiocyanate help stored electrons in Ag to be further transferred via the Ag-SCN ad-layer (the inner Helmholtz layer) to enhance the overall reduction of protons to molecular hydrogen (see Scheme 1). The Ag NP has a larger capacity for electron storage than Pt and Au NP but the discharge of stored electrons to the electrolyte is slower on Ag.[30,31] Therefore, the role of thiocyanate to accelerate the electron transfer and to facilitate the proton reduction is critical on the silver surface. This explanation is consistent with the PEC analysis results which showed that the presence of thiocyanate on the Ag/TiO_2 electrode reduced the over-

potential of H_2 production and the electron transfer resistance. Moreover, the fact that the dark stationary potential of Ag/TiO_2 shifted more positively upon adding thiocyanate is consistent with the view that the ad-layer of Ag-SCN attracts protons.

4. CONCLUSION

The presence of thiocyanate in the aqueous suspension of Ag/TiO_2 greatly enhanced (~4 times) the photocatalytic production of H_2, although the thiocyanate itself apparently
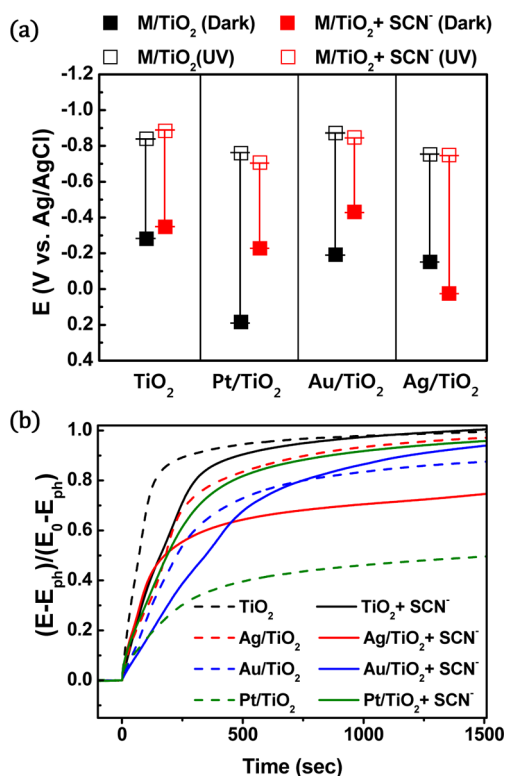
Figure 7. (a) Open-circuit stationary values of bare TiO_2 and M/TiO_2 (M = Pt, Au, and Ag) in the dark (E_0, filled squares) and under illumination (E_{ph}, open squares) with and without thiocyanate. (b) Normalized open-circuit potential relaxation, upon turning off the UV light incident on the M/TiO_2 electrode in the absence and presence of KSCN (0.1 mM). [$NaClO_4$] = 0.2 M, pH = 11.0, electrode area of 1 cm^2, λ > 320 nm.

Scheme 1. Illustration of the Photocatalytic Mechanism for H_2 Production Mediated by the Ag-SCN Functional Groups on TiO_2
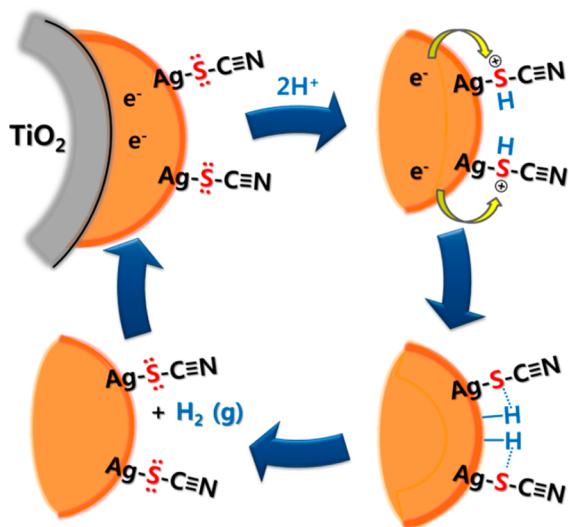
remained unreacted during the photoirradiation. The photocatalytic activity of $Ag/TiO_2/SCN$ system was maintained through the multiple cycles of photoreactions. The positive effect of thiocyanate was uniquely observed only with the Ag system, not with Pt and Au systems. This provides a simple method of boosting up the catalytic H_2 production activity of

silver, which has much lower material cost than more active and popular noble metal catalysts such as Pt and Au. Thiocyanate anion was selectively complexed on the surface of Ag NPs, which was confirmed by Raman spectral analysis and spot-profile EDS analysis. The formation of Ag-SCN surface complex enhances the interfacial electron transfer rate and facilitates the adsorption of protons on silver surface, which subsequently enhances the H_2 production on Ag/TiO_2. This study demonstrates a very simple method of making silver more catalytic for the production of H_2 under solar radiation. Although the overall activity of the $Ag/TiO_2/SCN$ system is still lower than that of Pt/TiO_2 and Au/TiO_2 for H_2 production, this new phenomenon may provide a valuable clue for how the low catalytic activity of silver can be overcome. The thiocyanate effect can make silver a more competitive substitute for more expensive noble metals. This is particularly important when the overall material cost is taken into account in evaluating the total cost efficiency of the solar hydrogen production method.

■ ASSOCIATED CONTENT

S **Supporting Information**

The Supporting Information is available free of charge on the ACS Publications website at DOI: 10.1021/acscatal.5b02376.

> Rates of H_2 generation with and STEM images for Pt/TiO_2, Au/TiO_2, and Ag/TiO_2; the original spot profile EDS spectra; X-ray photoelectron spectra (XPS) of the silver band in Ag/TiO_2 adsorbed with SCN^- (PDF)

■ AUTHOR INFORMATION

Corresponding Author
*E-mail: wchoi@postech.edu.

Notes
The authors declare no competing financial interest.

■ ACKNOWLEDGMENTS

■ REFERENCES

(1) Chen, X.; Shen, S.; Guo, L.; Mao, S. S. *Chem. Rev.* **2010**, *110*, 6503−6570.
(2) Faber, M. S.; Jin, S. *Energy Environ. Sci.* **2014**, *7*, 3519−3542.
(3) Takata, T.; Pan, C. S.; Nakabayashi, M.; Shibata, N.; Domen, K. *J. Am. Chem. Soc.* **2015**, *137*, 9627−9634.
(4) Maeda, K. *ACS Catal.* **2013**, *3*, 1486−1503.
(5) Fujishima, A.; Honda, K. *Nature* **1972**, *238*, 37−38.
(6) Hoffmann, M. R.; Martin, S. T.; Choi, W.; Bahnemann, D. W. *Chem. Rev.* **1995**, *95*, 69−96.
(7) Schneider, J.; Matsuoka, M.; Takeuchi, M.; Zhang, J. L.; Horiuchi, Y.; Anpo, M.; Bahnemann, D. W. *Chem. Rev.* **2014**, *114*, 9919−9986.
(8) Kim, H. I.; Monllor-Satoca, D.; Kim, W.; Choi, W. *Energy Environ. Sci.* **2015**, *8*, 247−257.
(9) Cai, J.; Zhu, Y.; Liu, D.; Meng, M.; Hu, Z.; Jiang, Z. *ACS Catal.* **2015**, *5*, 1708−1716.
(10) Li, C.; Koenigsmann, C.; Ding, W.; Rudshteyn, B.; Yang, K. R.; Regan, K. P.; Konezny, S. J.; Batista, V. S.; Brudvig, G. W.; Schmuttenmaer, C. A.; Kim, J. H. *J. Am. Chem. Soc.* **2015**, *137*, 1520−1529.

(11) Tang, J.; Durrant, J. R.; Klug, D. R. *J. Am. Chem. Soc.* **2008**, *130*, 13885−13891.

(12) Bai, S.; Jiang, J.; Zhang, Q.; Xiong, Y. *Chem. Soc. Rev.* **2015**, *44*, 2893−2939.

(13) Schweinberger, F. F.; Berr, M. J.; Doblinger, M.; Wolff, C.; Sanwald, K. E.; Crampton, A. S.; Ridge, C. J.; Jackel, F.; Feldmann, J.; Tschurl, M.; Heiz, U. *J. Am. Chem. Soc.* **2013**, *135*, 13262−13265.

(14) Hirakawa, T.; Kamat, P. V. *J. Am. Chem. Soc.* **2005**, *127*, 3928−3934.

(15) Khan, M. R.; Chuan, T. W.; Yousuf, A.; Chowdhury, M. N. K.; Cheng, C. K. *Catal. Sci. Technol.* **2015**, *5*, 2522−2531.

(16) Ding, D.; Liu, K.; He, S.; Gao, C.; Yin, Y. *Nano Lett.* **2014**, *14*, 6731−6736.

(17) Xie, F.; Choy, W. C. H.; Sha, W. E. I.; Zhang, D.; Zhang, S.; Li, X.; Leung, C. W.; Hou, J. *Energy Environ. Sci.* **2013**, *6*, 3372−3379.

(18) Murdoch, M.; Waterhouse, G. I. N.; Nadeem, M. A.; Metson, J. B.; Keane, M. A.; Howe, R. F.; Llorca, J.; Idriss, H. *Nat. Chem.* **2011**, *3*, 489−492.

(19) Su, R.; Tiruvalam, R.; Logsdail, A. J.; He, Q.; Downing, C. A.; Jensen, M. T.; Dimitratos, N.; Kesavan, L.; Wells, P. P.; Bechstein, R.; Jensen, H. H.; Wendt, S.; Catlow, C. R. A.; Kiely, C. J.; Hutchings, G. J.; Besenbacher, F. *ACS Nano* **2014**, *8*, 3490−3497.

(20) Park, J.; Yi, J.; Tachikawa, T.; Majima, T.; Choi, W. *J. Phys. Chem. Lett.* **2010**, *1*, 1351−1355.

(21) Park, H.; Kim, H.-i.; Moon, G.-h.; Choi, W. *Energy Environ. Sci.* **2016**, DOI: 10.1039/C5EE02575C.

(22) Yang, Y. Z.; Chang, C. H.; Idriss, H. *Appl. Catal., B* **2006**, *67*, 217−222.

(23) He, D.; Jiao, X.; Jiang, P.; Wang, J.; Xu, B. Q. *Green Chem.* **2012**, *14*, 111−116.

(24) Maijenburg, A. W.; Veerbeek, J.; de Putter, R.; Veldhuis, S. A.; Zoontjes, M. G. C.; Mul, G.; Montero-Moreno, J. M.; Nielsch, K.; Schafer, H.; Steinhart, M.; ten Elshof, J. E. *J. Mater. Chem. A* **2014**, *2*, 2648−2656.

(25) Wang, F.; Jiang, Y.; Lawes, D. J.; Ball, G. E.; Zhou, C.; Liu, Z.; Amal, R. *ACS Catal.* **2015**, *5*, 3924−3931.

(26) Tsukamoto, D.; Shiro, A.; Shiraishi, Y.; Sugano, Y.; Ichikawa, S.; Tanaka, S.; Hirai, T. *ACS Catal.* **2012**, *2*, 599−603.

(27) Linsebigler, A. L.; Lu, G.; Yates, J. T. *Chem. Rev.* **1995**, *95*, 735−758.

(28) Kim, J.; Monllor-Satoca, D.; Choi, W. *Energy Environ. Sci.* **2012**, *5*, 7647−7656.

(29) Walter, M. G.; Warren, E. L.; McKone, J. R.; Boettcher, S. W.; Mi, Q. X.; Santori, E. A.; Lewis, N. S. *Chem. Rev.* **2010**, *110*, 6446−6473.

(30) Takai, A.; Kamat, P. V. *ACS Nano* **2011**, *5*, 7369−7376.

(31) Wood, A.; Giersig, M.; Mulvaney, P. *J. Phys. Chem. B* **2001**, *105*, 8810−8815.

(32) Choi, H.; Chen, W. T.; Kamat, P. V. *ACS Nano* **2012**, *6*, 4418−4427.

(33) El Badawy, A. M.; Luxton, T. P.; Silva, R. G.; Scheckel, K. G.; Suidan, M. T.; Tolaymat, T. M. *Environ. Sci. Technol.* **2010**, *44*, 1260−1266.

(34) Levard, C.; Hotze, E. M.; Colman, B. P.; Dale, A. L.; Truong, L.; Yang, X. Y.; Bone, A.; Brown, G. E.; Tanguay, R. L.; Di Giulio, R. T.; Bernhardt, E. S.; Meyer, J. N.; Wiesner, M. R.; Lowry, G. V. *Environ. Sci. Technol.* **2013**, *47*, 13440−13448.

(35) Levard, C.; Reinsch, B. C.; Michel, F. M.; Oumahi, C.; Lowry, G. V.; Brown, G. E. *Environ. Sci. Technol.* **2011**, *45*, 5260−5266.

(36) Park, J.; Choi, I.; Kim, Y.; Yi, J. *Bull. Korean Chem. Soc.* **2011**, *32*, 3433−3436.

(37) Park, G.; Lee, C.; Seo, D.; Song, H. *Langmuir* **2012**, *28*, 9003−9009.

(38) Wang, C.; Liu, C.; Wang, M.; Shen, T. *Spectrochim. Acta, Part A* **1999**, *55*, 991−998.

(39) Park, Y.; Kang, S. H.; Choi, W. *Phys. Chem. Chem. Phys.* **2011**, *13*, 9425−9431.

(40) Byrne, J. A.; Eggins, B. R.; Brown, N. M. D.; McKinney, B.; Rouse, M. *Appl. Catal., B* **1998**, *17*, 25−36.

(41) Berger, T.; Monllor-Satoca, D.; Jankulovska, M.; Lana-Villarreal, T.; Gomez, R. *ChemPhysChem* **2012**, *13*, 2824−2875.

(42) Kamat, P. V. *Langmuir* **1985**, *1*, 608−611.

(43) Bahnemann, D. W.; Henglein, A.; Lilie, J.; Spanhel, L. *J. Phys. Chem.* **1984**, *88*, 709−711.

(44) Pendlebury, S. R.; Barroso, M.; Cowan, A. J.; Sivula, K.; Tang, J.; Gratzel, M.; Klug, D.; Durrant, J. R. *Chem. Commun.* **2011**, *47*, 716−718.

(45) Tuschel, D. *Spectroscopy* **2014**, *29*, 14−22.

(46) Henglein, A.; Meisel, D. *J. Phys. Chem. B* **1998**, *102*, 8364−8366.

(47) Durga Praveena, V.; K, V. K. *Int. J. Innov. Sci. Eng. Technol.* **2015**, *2*, 741−752.

(48) Monllor-Satoca, D.; Gomez, R.; Choi, W. *Environ. Sci. Technol.* **2012**, *46*, 5519−5527.

(49) Luque, A.; Martí, A.; López, N.; Antolín, E.; Cánovas, E.; Stanley, C.; Farmer, C.; Caballero, L. J.; Cuadra, L.; Balenzategui, J. L. *Appl. Phys. Lett.* **2005**, *87*, 083505.

(50) Monllor-Satoca, D.; Gomez, R. *J. Phys. Chem. C* **2008**, *112*, 139−147.